A Discretized Population Balance for Continuous Systems at Steady State

This paper is concerned with the solution of the population balance for continuous systems at steady state, in which the active mechanisms are nucleation, growth and aggregation. A discretized population balance, initially proposed by Hounslow et al. (1988a) for batch systems, is adapted for use with continuous systems at steady state. It is shown that simultaneous nucleation and growth can be described very effectively by the discrete equations. Criteria are developed for the selection of the optimal size domain. A simple modification to the original discrete equations describing growth, permits the modelling of size-dependent growth effects. Both size-independent and size-dependent aggregation are described by the discrete equations with three significant-figure accuracy. The complete set of discrete equations is used to simulate the nucleation, growth and aggregation of Nickel Ammonium Sulphate. It is shown that analysis by the approximate model must lead to underestimation of the nucleation and growth rates.

Michael J. Hounslow
Department of Chemical Engineering
The University of Adelaide
Adelaide, South Australia 5001

Introduction

The description of systems in which suspensions of particles undergo simultaneous nucleation, growth and aggregation is fraught with difficulty. Simply writing down the relationship that describes the conservation of particle numbers presents difficulties; the resulting equation is frequently of a nonlinear integro-partial-differential type, in two or more dimensions. This equation of particle-number continuity is known as the population balance.

While the population balance itself is often complex, its solution by analytical means is frequently, indeed normally, impossible. As an illustration of this fact, one may reflect that the simplest possible system, the well mixed vessel at steady state, is described by a population balance that, with all three mechanisms active, cannot, to the author's knowledge, be solved analytically.

This paper is concerned with the study of this simplest possible system. Specifically, the uses of a discretized form of the population balance will be investigated. In this approach the particle-size distribution is broken up into a number of discrete size ranges and the integro-differential equation of the analytical population balance is replaced by a series of algebraic equations, one for each size range.

Theory

The credit for introducing the mathematical formalism of the population balance approach is generally attributed to Hulburt and Katz (1961), who sought, in writing that paper, to apply a statistical-mechanical view to the conservation laws governing the size distributions of particulate systems. Since the publication of their pioneering paper there have been many contributors to the literature of the field. Perhaps best known are the works of Randolph and Larson, as exemplified by their book (1988), and of Ramkrishna (1985).

The population balance is, in effect, a statement of continuity for particulate systems. In qualitative terms it states that the rate of increase of the number of particles of a certain size must be related to the rate at which particles of that size are being formed and removed, by so-called birth and death processes, and the rate at which particles are growing. The "number of particles of a certain size" is expressed as a population density, n. The population density at a size, L, $n(L)$ is defined as the ratio of the number of particles, dN, in a differential neighborhood around L, to the size of the neighborhood, dL. That is,

$$n(L) = \frac{dN}{dL} \tag{1}$$

It follows that $N(L)$ is the number of particles less than size L. It is usual to express n and N on some convenient volumetric basis, such as per litre or per reactor volume.

For a continuous system of constant volume, Randolph and

Larson give the population balance as

$$\frac{\partial n}{\partial t} + \frac{\partial (Gn)}{\partial L} = B - D + \frac{1}{V}(\Sigma Q_{in} n_{in} - \Sigma Q_{out} n_{out}) \quad (2)$$

This statement of continuity in particle phase-space relates the rate of accumulation, $\partial n/\partial t$, the convective flux along the size axis, $\partial(Gn)/\partial L$, the birth and death rates, B and D, and the bulk flow into and out of the system. G is the growth rate and may be a function of size.

The birth and death rates might include terms for such phenomena as nucleation, aggregation, and breakage. Only the first two of these phenomena are considered here, the appropriate formulations for which are given by

$$B(L) = B_0 \delta(L) \quad \text{Nucleation} \quad (3)$$

$$B(L) = \frac{L^2}{2} \int_0^L \frac{\beta((L^3 - \lambda^3)^{1/3}, \lambda) n((L^3 - \lambda^3)^{1/3}) n(\lambda)}{(L^3 - \lambda^3)^{2/3}} d\lambda$$

$$D(L) = n(L) \int_0^\infty \beta(L, \lambda) n(\lambda) d\lambda \quad \text{Aggregation} \quad (4)$$

In these expressions, B_0 is the nucleation rate and β the aggregation kernel, which, like the growth rate, may be a function of particle size.

For the case of a continuous, mixed-suspension, mixed-product-removal crystallizer (CMSMPRC), at steady state, Eq. 2 reduces to

$$\frac{\partial (Gn)}{\partial L} = B - D + \frac{n_{in} - n}{\tau} \quad (5)$$

In this last equation, τ, the draw-down time, is defined by $\tau = V/Q$. With all its terms included, Eq. 5 cannot be solved analytically. However, before proceeding to numerical solutions, one further approach may be considered.

The moments of a particle-size distribution are defined by

$$m_j = \int_0^\infty L^j n(L)\, dL$$

Under many circumstances, Eq. 5 may be transformed into a series of algebraic equations relating a closed set of moments which may be solved relatively easily.

Discretized Population Balance

The complexity of the continuous population balance, formed by combining Eqs. 3–5, has led many authors to seek an alternative approach, in which the population balance is cast in terms of quantity of material in each of a number of discrete size ranges. These discretized population balances vary from a simple description of batch aggregation by Batterham et al. (1981), posed in terms of the number of particles in a size interval, through descriptions of batch growth and aggregation by Marchal et al. (1988), again posed in terms of particle number, to the generalized work of Gelbard and Seinfeld (1980) and Gelbard et al. (1980). The last named authors write their discretized population balance (DPB) in terms of an arbitrary integral property of an interval, which might be particle number, volume, or any other similar quantity. The approach also allows the use of an arbitrary internal coordinate, which might, perhaps, be particle size or mass. As a consequence of its flexibility, this last approach requires the evaluation of some nine double integrals for the aggregation terms and three ordinary integrals for the growth terms.

In a previous paper, Hounslow et al. (1988a), the author has shown that the approaches of Batterham et al. and of Marchal et al. lead to erroneous solutions; each systematically overestimating the rate of change of the moments of the size distribution. It may also be shown that the application of Gelbard and Seinfeld's method to size-independent aggregation and growth, yields a set of equations inconsistent with the analytical moment form of the population balance.

To overcome the inconsistency concerning moments, Hounslow et al. (1988a) developed a DPB for batch systems which is guaranteed to predict the correct rate of change for the first three or four moments. All the coefficients in the resulting equations are constants; no integration is required. The rest of this paper is concerned principally with applying their approach to continuous steady-state systems.

For a well-mixed vessel the mass balance for any conserved property, ζ, requires that

$$V \frac{d\zeta}{dt} = V \dot{\zeta}(\underline{x}) + \Sigma Q_{in} \zeta_{in} - \Sigma Q_{out} \zeta_{out} \quad (6)$$

where $\dot{\zeta}(\underline{x})$ is the net rate of generation of ζ under the conditions prevailing in the vessel, as described by the coordinate vector, $\underline{x}$. One may note at once that the rate of change of ζ in a batch system, that is, one for which $Q_{in} = Q_{out} = 0$, must be given by

$$\left(\frac{d\zeta}{dt}\right)_{Batch} = \dot{\zeta}(\underline{x}) \quad (7)$$

For the case of a CMSMPRC at steady state, with one stream entering and one stream leaving, Eq. 6 becomes

$$0 = \dot{\zeta}(\underline{x}) + \frac{\zeta_{in} - \zeta}{\tau} \quad (8)$$

Combining Eqs. 7 and 8, and recognizing that the conserved property of interest is N_i, the number of particles in the i^{th} size

interval, we may write the DPB for a CMSMPRC at steady state.

$$\left(\frac{dN_i}{dt}\right)_{\text{Batch}} = \frac{N_i - N_{i,\text{in}}}{\tau} \tag{9}$$

In this work, the left hand side is made up of three terms:

$$\left(\frac{dN_i}{dt}\right)_{\text{Batch}} = \left(\frac{dN_i}{dt}\right)_{\text{Nucleation}} + \left(\frac{dN_i}{dt}\right)_{\text{Growth}} + \left(\frac{dN_i}{dt}\right)_{\text{Aggregation}} \tag{10}$$

which, in a previous paper by the author, Hounslow et al. (1988a), have been determined to be

$$\left(\frac{dN_i}{dt}\right)_{\text{Aggregation}} = N_{i-1}\sum_{j=1}^{i-2} 2^{j-i+1}\beta_{i-1,j}N_j + \frac{1}{2}\beta_{i-1,i-1}N_{i-1}^2 - N_i\sum_{j=1}^{i-1} 2^{j-i}\beta_{i,j}N_j - N_i\sum_{j=1}^{\infty}\beta_{i,j}N_j \tag{11}$$

$$\left(\frac{dN_i}{dt}\right)_{\text{Growth}} = \frac{2G}{(1+r)L_i} \cdot \left(\frac{r}{r^2-1}N_{i-1} + N_i - \frac{r}{r^2-1}N_{i+1}\right) \tag{12}$$

$$\left(\frac{dN_i}{dt}\right)_{\text{Nucleation}} = \begin{cases} B_0 & i = 1 \\ 0 & i \neq 1 \end{cases} \tag{13}$$

Hounslow et al. also showed that the jth moment may be calculated by

$$m_j = \sum_i \left(\frac{1+r}{2}L_i\right)^j N_i \tag{14}$$

In what follows, the DPB, Eq. 9, will be compared with its continuous analogue, Eq. 5. The method to be adopted is one of conducting the investigation mechanism by mechanism, and then considering a case study in which all the mechanisms are active.

Methods

The solution of the DPB requires that a number of nonlinear algebraic equations, typically thirty to forty, be solved in conjunction with whatever side conditions are required, such as species conservation laws. The equation-oriented flowsheeting package, SpeedUp, provides an ideal computing environment for such a task. For a description of SpeedUp see, for example, Sargent et al. (1982) or Prosys Technology Ltd. (1988).

The DPB, Eq. 9, and the moment-generating equation, Eq. 14, were coded as SpeedUp procedures called by Models that contained all the remaining auxiliary equations. The numerical calculations presented in this paper were produced using SpeedUp, including the parameter estimation results presented in a later section. For details of the SpeedUp implementation of the DPB, see Hounslow (1989).

Nucleation and Growth

Any meaningful investigation of nucleation in a CMSMPRC requires that growth takes place simultaneously. The DPB to be considered is formed by combining Eqs. 12 and 13 with 9, although it should be pointed out that Eq. 12 will later be modified to deal with size-dependent growth rates.

Size-independent growth

The production of crystals by simultaneous nucleation and growth in a well-mixed reactor provides an ideal starting point for the investigation at hand, not least as a consequence of the ease with which an analytical solution is found. The well-known exponential size distribution produced in these circumstances, given, for example, by Randolph and Larson (1988), is

$$n(L) = \frac{B_0}{G}\exp\left(\frac{-L}{G\tau}\right) \tag{15}$$

Defining a dimensionless length, $x = L/G\tau$, and the normalized density function, $f = (n/m_0)(dL/dx)$, Eq. 15 becomes

$$f(x) = e^{-x} \tag{16}$$

As a basis for comparison, this last result could hardly be simpler.

Turning now to the set of discrete equations to be compared with Eq. 16. The DPB becomes

$$\begin{aligned} 0 &= \frac{G}{L_1}(bN_1 + cN_2) - \frac{N_1}{\tau} + B_0 \\ 0 &= \frac{G}{L_i}(aN_{i-1} + bN_i + cN_{i+1}) - \frac{N_i}{\tau} \qquad i > 1 \end{aligned} \tag{17}$$

where

$$a = \frac{2r}{(1+r)(r^2-1)}, \quad b = \frac{2}{1+r}, \quad \text{and} \quad c = \frac{-2r}{(1+r)(r^2-1)}$$

In dimensionless forms, with $\tilde{N}_i = N_i/m_0$, this family of equations becomes

$$\begin{bmatrix} b-x_1 & c & & & & \\ a & b-x_2 & c & & & \\ & a & b-x_3 & c & & \\ & & \ddots & \ddots & \ddots & \\ & & & a & b-x_{n_{eq}-1} & c \\ & & & & a & b-x_{n_{eq}} \end{bmatrix} \begin{bmatrix} \tilde{N}_1 \\ \tilde{N}_2 \\ \vdots \\ \tilde{N}_{eq} \end{bmatrix} = \begin{bmatrix} x_1 \\ 0 \\ \vdots \\ 0 \end{bmatrix}$$

In solving this set of equations, values must be assigned to two parameters, which together define the size domain considered. The parameters are the minimum size, x_1, and the number of discrete equations considered, n_{eq}. In choosing a finite size domain there must inevitably be an associated error brought about by a failure to count those particles outside the domain. This error, termed the finite domain error (FDE) by Gelbard and Seinfeld (1978), may be calculated for the analytical solution, Eq. 16, as

$$\text{FDE} = 1 - \exp(-x_1) + \exp(-x_1 r^{n_{eq}}) \tag{18}$$

It follows that for any value of n_{eq} there is a value for x_1 that minimizes the FDE.

$$x_1^{opt} = \frac{n_{eq} \ln(r)}{r_{eq}^n - 1} \tag{19}$$

Using Eqs. 18 and 19, the values in Table 1 may be deduced.

From the data displayed in Table 1, it may be seen that a discretized domain comprising ten size intervals, and thus covering a 10:1 range of particle size, fails to include 30.1% of all the crystals formed. If the FDE is to be less than 0.1%, some 40 size intervals must be used.

Figure 1 compares the analytical solution available from Eq. 16 with the numerical solution of Eq. 17, using $x_1 = 0.001$ and $n_{eq} = 40$. It is clear that the numerical solution is in excellent agreement with the analytical solution. It is worth noting that at every interval the numerical solution is slightly greater than the analytical solution. This result flows directly from the FDE. Given that the parameters, a, b, c, have been chosen to predict the rate of change of total numbers, N_T, exactly, $N_i \geq 0$, and FDE > 0, it follows that the particles that should be found outside the discretized size domain *must* be assigned, erroneously, to size intervals within the domain.

There is a further issue to be canvassed in the selection of the discrete size domain. When very small values of x_1 are used, the numerical solution yields oscillatory values of N_i for small i. In order to examine this artifact, the following sum of square error (SSE) parameter was defined.

$$\text{SSE}_5 = \sum_{i=1}^{5} \left(\tilde{N}_i^{\text{numerical}} - \tilde{N}_i^{\text{analytical}} \right)^2 \tag{20}$$

Figure 2 is a pseudo-three-dimensional plot of SSE_5 vs. n_{eq} and x_1. From this plot it is apparent that there is a very clearly defined no-go region in which inaccurate solutions are obtained. By observation, negligible error is incurred while

$$x_1 > 1.64 \exp\left(\frac{-n_{eq}}{5.46}\right) \tag{21}$$

Table 1. Optimum Size Domain

n_{eq}	x_1^{opt}	$\text{FDE}_{min} \times 100\%$
10	0.254	30.1
20	0.0459	5.43
30	0.00678	0.772
40	0.000895	0.099
50	0.0001111	0.012

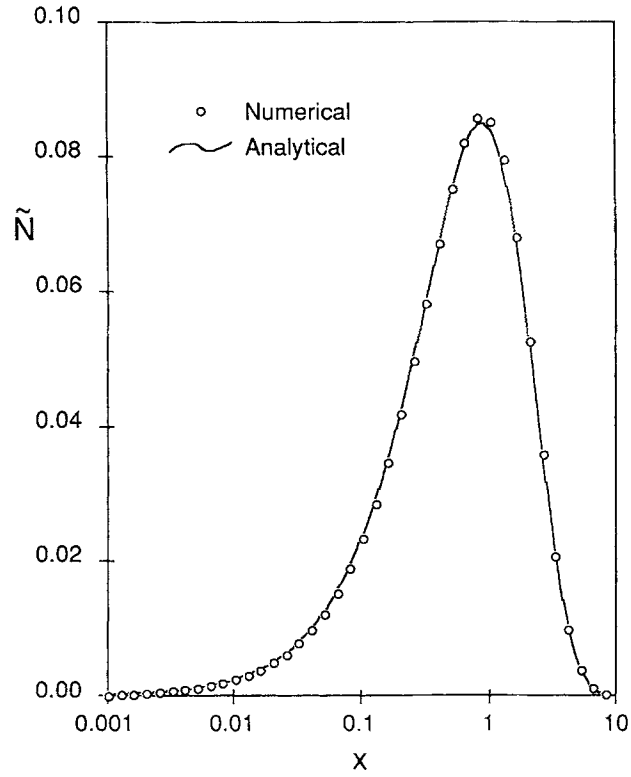

Figure 1. Numerical and analytical solutions to the population balance with simultaneous nucleation and size-independent growth.

The values given by this last equation are essentially equal to x_1^{opt}. Consequently, optimal choice of x_1 avoids the oscillatory artifact.

Provided an appropriate finite domain is selected, the DPB, given by the tridiagonal set of equations, Eq. 17, yields a size distribution indistinguishable from the well-known analytical result, Eq. 15.

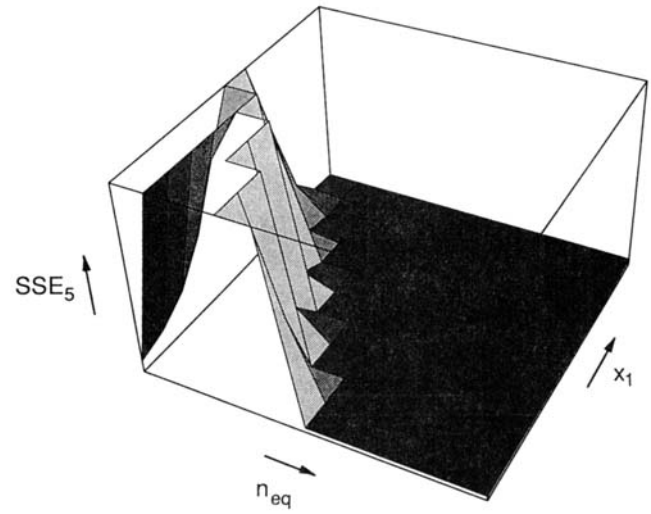

Figure 2. Error in predicting fine-particle numbers vs. the finite size domain.

Size-dependent growth

Hitherto, this discussion has proceeded on the basis that the linear rate of growth, G, is independent of size. While in many crystallization studies this assumption is justified, it has long been contended that in some systems the growth rate is a function of size. Further, in studies of aerosol dynamics it is often found that the rate of condensation implies a size-dependent growth rate.

There is a further reason for wishing to extend this analysis to systems in which the growth rate varies from interval to interval. Many of the systems that were previously thought to be consistent with a size-dependent growth mechanism are now understood to be better described by the phenomenon of growth rate dispersion. In such systems, individual crystals apparently have some kind of intrinsic activity, which inclines some to grow faster than the average, and some to grow slower. In effect, the population density is no longer a function of one internal coordinate, perhaps length, but depends on at least one other characteristic—the activity. In the context of a one-dimensional DPB, this phenomenon manifests itself as a variation in growth rate from interval to interval: as more active crystals grow into the larger size intervals, the growth rate in those intervals will increase. One might easily envisage some computational scheme which keeps track of the variation in activity in each interval, and adjusts the growth rate accordingly. In the present work, however, we seek only to extend the analysis to systems where the variation in growth rate can be given explicitly.

The simple device of replacing G with G_i in Eq. 12, yields, for the batch case,

$$\left(\frac{dN_i}{dt}\right)_{\text{Batch}} = \frac{G_i}{L_i}(aN_{i-1} + bN_i + cN_{i+1}) \tag{22}$$

An assessment of this formulation may be made by investigating the rate of change of the zeroth moment, which should be zero.

$$\left(\frac{dm_0}{dt}\right)_{\text{Batch}} = \sum_{i=1}^{\infty} \frac{G_i}{L_i}(aN_{i-1} + b\,N_i + cN_{i+1})$$

$$= \sum_{i=1}^{\infty} \left(\frac{1+r}{2}\right)^j L_i^{-1} N_i \left(\frac{a}{r} G_{i+1} + bG_i + crG_{i-1}\right)$$

This last expression is not equal to zero for arbitrary G_i, and thus the approach of Eq. 22 must be rejected. As an alternative, consider the expression below.

$$\left(\frac{dN_i}{dt}\right)_{\text{Batch}} = \frac{1}{L_i}(aG_{i-1}N_{i-1} + bG_iN_i + cG_{i+1}N_{i+1}) \tag{23}$$

For this expression, the rate of change of the zeroth moment is given by

$$\left(\frac{dm_0}{dt}\right)_{\text{Batch}} = \sum_{i=1}^{\infty} \frac{1}{L_i}(aG_{i-1}N_{i-1} + bG_iN_i + cG_{i+1}N_{i+1})$$

$$= \sum_i \frac{G_i}{L_i} N_i \left(\frac{a}{r} + b + cr\right)$$

$$= 0$$

This last result arises from the original choice of a, b, and c; one of the criteria for their selection was that $a/r + b + cr = 0$.

Let us now consider a particular form of the size dependence of growth. Abegg et al. (1968) propose that growth rate and size be related by

$$G = G_0(1 + \gamma L)^b \tag{24}$$

For the special case of $\gamma = 1/G_0\tau$, Randolph and Larson present a solution to the population balance for a CMSMPRC:

$$f(x) = \frac{1}{(1+x)^b} \exp\left[\frac{1 - (1+x)^{1-b}}{1-b}\right] \tag{25}$$

from which the dimensionless number in each size range may be deduced:

$$\tilde{N} = \exp\left[\frac{1 - (1+x)^{1-b}}{1-b}\right] - \exp\left[\frac{1 - (1+rx)^{1-b}}{1-b}\right] \tag{26}$$

The dimensionless moments are defined by

$$\tilde{m}_0 = \int_0^{\infty} x^j f(x)\, dx \tag{27}$$

For any value of j, the moment is given by

$$\tilde{m}_j = e^{1/1-b} \sum_{k=0}^{j} \left((-1)^{k+j}\binom{j}{k}(1-b)^{k/1-b}\Gamma\left[\frac{k+1-b}{1-b}, \frac{1}{1-b}\right]\right) \tag{28}$$

where $\Gamma(a, x)$ is the incomplete gamma function, and $\binom{j}{k}$ is the binomial coefficient, defined respectively by

$$\Gamma(a, x) = \int_x^{\infty} e^{-t} t^{a-1}\, dt \quad \text{and} \quad \binom{j}{k} = \frac{j!}{(j-k)!k!}$$

A series of simulations was conducted using the growth size-dependence of Abegg et al. The size distributions produced by the simulations are compared in Figure 3 with the analytical distributions given by Eq. 26. In Figure 4, the moments are compared in a similar fashion.

Both plots show the numerical results to be in close agreement with the expected analytical solution. The size distributions match best for high values of b and the lower moments are in better agreement than the higher moments, particularly at high values of b. The reasons for this behavior become apparent when the finite domain error is considered. Partly for reasons of convenience, and partly to illustrate this point, all the simulations presented in Figures 3 and 4 were conducted with $x_1 = 0.005$ and $n_{eq} = 40$. For small values of b, the optimum value of x_1 must be near the value calculated in Table 1, for size-independent growth, $x_1^{opt} = 0.000895$. So, for small values of b, by the argument given in the previous section, the numerical values for $\tilde{N}_i$ must be greater than the analytical values. However, as b is increased, the size distribution is skewed further and further to the right, diminishing the FDE, and thus diminishing the discrepancy between the numerical and analytical solutions.

To explain the discrepancy in the higher moments, one must reflect on the definition used for FDE. The definition used in

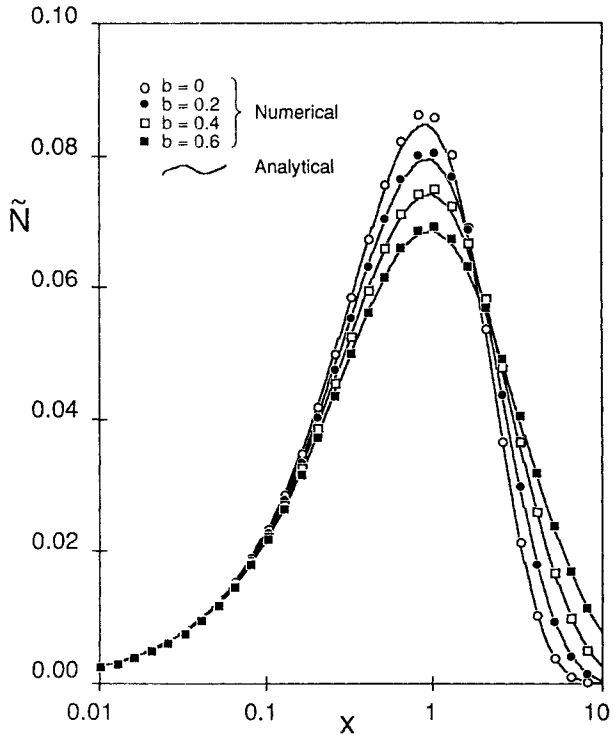

Figure 3. Particle-size distributions for size-dependent growth.

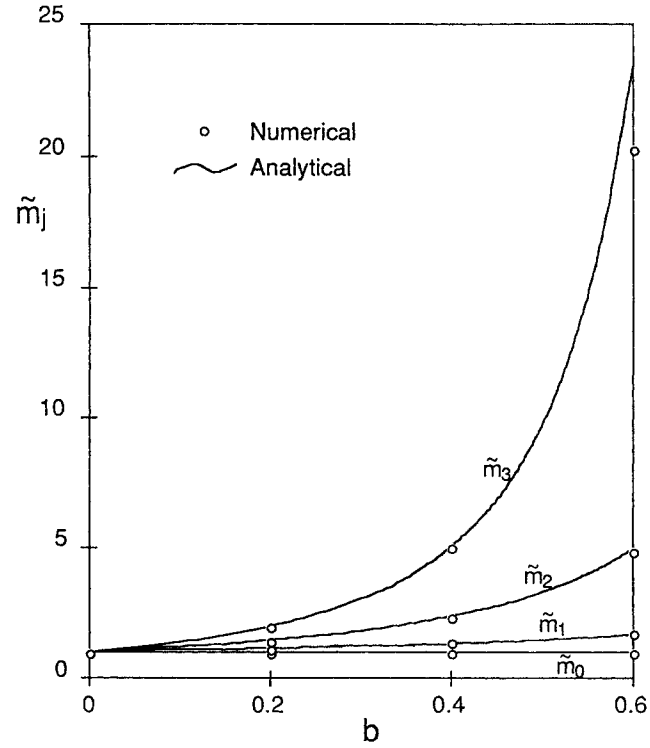

Figure 4. Moments of the particle-size distribution for size-dependent growth.

this work has been based on the number of particles that should be found outside the discrete domain, rather than, say, the volume of particles. Were a volume-sensitive FDE to be used, then the optimum value for x_1 must be increased, as a far greater error is incurred for failure to include the volume of a large particle than that of a small particle. Why then are the higher moments under-predicted? The discrete domain used in these simulations was selected to produce an acceptable FDE on a number basis. As a consequence, a small number (m_0), but a large volume (m_3) and area (m_2), of particles are excluded from the domain. This phenomenon is most marked when the distribution is skewed furthest to the right, that is, for large values of b.

As with size-independent growth, the DPB yields results for size-dependent growth entirely in agreement with published analytical results.

Aggregation

Solutions of the population balance for systems involving aggregation are notoriously difficult to obtain. In dealing with systems for which the rate of crystal growth is either zero or negligible, it is usually profitable to recast Eq. 5 in terms of a number-density function that uses volume as the internal coordinate. The population balance becomes

$$0 = \frac{1}{2}\int_0^v \beta(v-\epsilon,\epsilon)n(v-\epsilon)n(\epsilon)\,d\epsilon - n(v)\int_0^\infty \beta(v,\epsilon)n(\epsilon)\,d\epsilon + \frac{n_i - n}{\tau} \quad (29)$$

Size-independent aggregation

For all but the simplest cases, Eq. 29 cannot be solved analytically. The search for analytical solutions to Eq. 29 is simplified if the aggregation kernel, β, is taken to be constant. Further simplification is made possible by the consideration of a simple form of the feed size distribution, such as that given by Eq. 30.

$$n_i = \frac{N_0}{v_0}\exp\left(\frac{-v}{v_0}\right) \quad (30)$$

By putting $x = v/v_0$ and $f(x) = n(v)v_0/N_0$ and $T = \beta_0 N_0 \tau$, and noting that

$$\int_0^\infty f(x)\,dx = \frac{\sqrt{1+2T}-1}{T},$$

we transform Eq. 29 to

$$0 = \frac{1}{2}\int_0^x f(x-\epsilon)f(\epsilon)\,d\epsilon - \left(\frac{\sqrt{1+2T}-1}{T}\right)f(x) + \frac{e^{-x}-f(x)}{T} \quad (31)$$

This equation is solved in Appendix 1 using Laplace transforms. Its solution is

$$f(x) = \frac{I_0\left[\frac{-Tx}{1+2T}\right] + I_1\left[\frac{-Tx}{1+2T}\right]}{\exp\left[\frac{-(1+T)x}{1+2T}\right]\sqrt{1+2T}} \quad (32)$$

where I_0 and I_1 are the modified Bessel functions of the first kind, of order zero and one, respectively.

In Figure 5, this last equation is compared with the numerical solution available by solving the steady-state form of the DPB. The analytical and numerical solutions for $\tilde{N}$ are identical, typically, to the third significant figure. For the data displayed in Figure 5, the RMS error is in the range 0.0005 to 0.001, that is 0.2 to 0.4% of the peak value. In this and the next section, $\tilde{N}$ is defined as

$$\tilde{N} = \int_x^{2x} f(x)\,dx = \frac{1}{N_0}\int_v^{2v} n(v)\,dv$$

As was the case with batch aggregation (Hounslow et al. 1988a) the DPB describes simple aggregation systems with great accuracy.

Size-dependent aggregation

As an example of size-dependent aggregation, consider the following aggregation kernel:

$$\beta(u, v) = (u + v)\beta_0 \tag{33}$$

The population balance becomes

$$0 = \frac{\beta_0}{2}\int_0^v vn(v - \epsilon)n(\epsilon)\,d\epsilon - n(v)\beta_0\int_0^\infty (v + \epsilon)n(\epsilon)\,d\epsilon + \frac{n_i - n}{\tau} \tag{34}$$

If, as in the previous section, we restrict our study to that of the aggregation of a feed containing particles with the size distribution given by Eq. 30, the population balance may be rewritten in nondimensional form

$$0 = \frac{1}{2}\int_0^x xf(x - \epsilon)f(\epsilon)\,d\epsilon - f(x)\int_0^\infty (x + \epsilon)f(\epsilon)\,d\epsilon + \frac{e^{-x} - f}{T} \tag{35}$$

where $T = v_0\beta_0 N_0\tau$. The second integral in the last equation is the sum of the zeroth and first moments of the dimensionless size distribution, f. Hence, Eq. 35 becomes

$$0 = \frac{1}{2}\int_0^x xf(x - \epsilon)f(\epsilon)\,d\epsilon - f(x)\left(\frac{x}{1 + T} + 1\right) + \frac{e^{-x} - f}{T} \tag{36}$$

The author is unaware of any analytical solution to this last equation and presents an approximate series solution in Appendix 2.

A number of simulations were conducted using the nonconstant kernel of Eq. 33, the numerical results from which are compared in Figure 6 with the series solution of Appendix 2. The numerical results are again in excellent agreement with the solution to the continuous population balance. The results for $T = 0.25$ show the greatest discrepancy, but the error almost

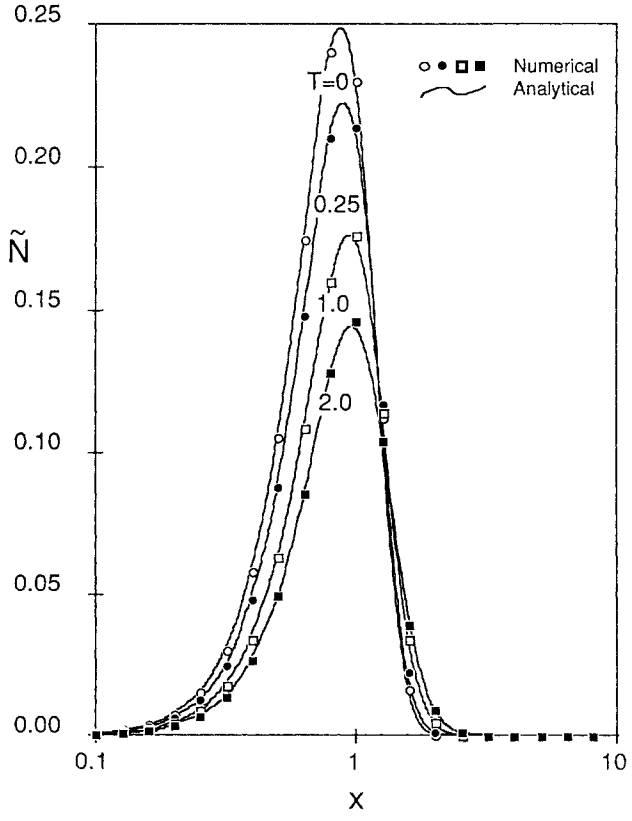

Figure 5. Particle-size distributions for size-independent aggregation.

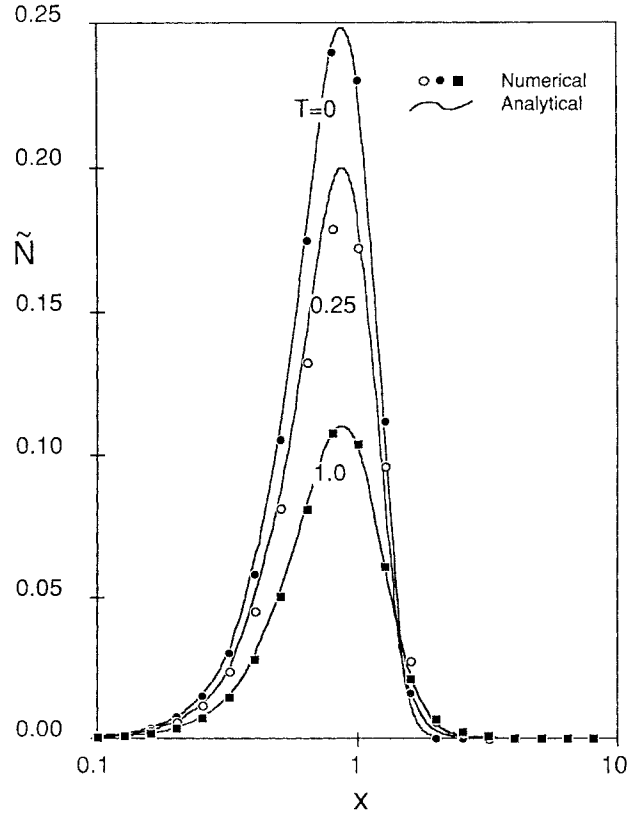

Figure 6. Particle-size distributions for size-dependent aggregation.

certainly lies in the series solution to the continuous population balance. There is no reason, *a priori*, to assume that the series solution is any more accurate than the numerical solution calculated from the DPB. However, given that the two solutions are so nearly coincident, and were generated by entirely independent means, there seems to be good reason to believe that both are correct.

Before proceeding, it is worth pausing to reflect on the quality of the results obtained from the DPB. From the evidence presented so far in this paper, coupled with that of the author's earlier paper, very reliable solutions are available for batch and continuous systems undergoing any nucleation, growth, and aggregation. In another paper by the author, Hounslow et al. (1988b), it is shown that batch experimental systems in which all three mechanisms are active are well described by the discrete form of the population balance. In the next section it is shown that a similar, but continuous rather than batch, system is also well described by the DPB.

Nucleation, Growth, and Aggregation

Tavare et al. (1985) present results from a study of the crystallization kinetics of Nickel Ammonium Sulphate (NAS) conducted in a CMSMPRC at steady state. The authors report that microscopic analysis of the crystallizer product revealed the presence of aggregates. The curvature evident in their semi-logarithmic plot of population density vs. crystal size is also characteristic of an aggregating system. Using the approximate analysis of Liao and Hulburt (1976), the authors attempt to quantify the growth and nucleation rates along with an aggregation parameter, A, which is analogous to the aggregation kernel considered here. The analysis of Liao and Hulburt is based on an approximation to the continuous population balance in which it is assumed that aggregation conserves total crystal length rather than volume.

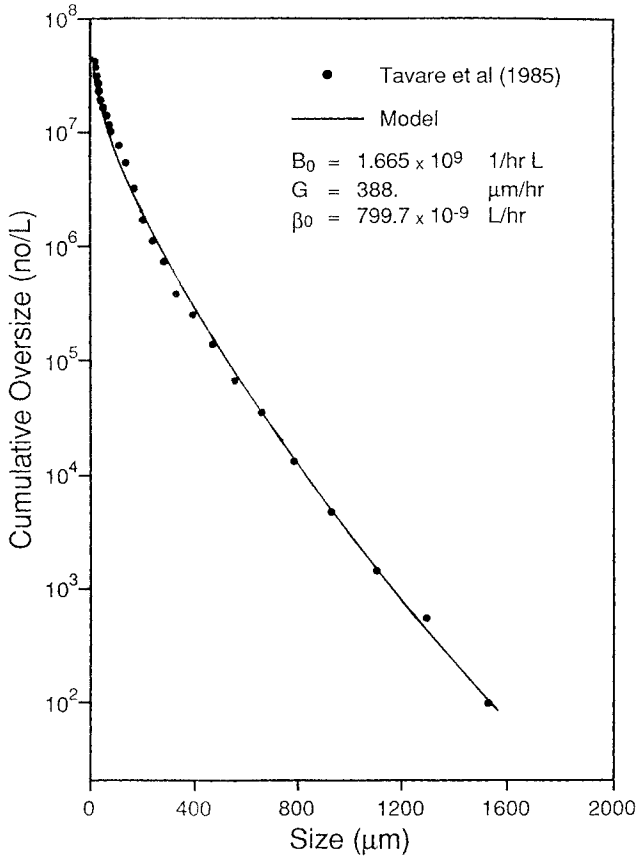

Figure 7. Experimental and fitted cumulative number oversize data for nickel ammonium sulphate.

In the present work, the data of Tavare et al. are reexamined by means of the DPB developed above, Eq. 9. The experimental conditions were modeled by a size-independent growth rate and aggregation kernel. SpeedUp's parameter estimation facilities were used to generate values for B_0, G and β_0 that minimized the sum of square error in the prediction of the logarithm of the cumulative oversize. Figure 7 displays experimental and fitted values for the cumulative oversize calculated with $B_0 = 1.665 \times 10^9$ 1/h · L, $G = 388$ μm/h and $\beta_0 = 800 \times 10^{-9}$ L/h.

The calculated and experimental distributions shown in Figure 7 are in excellent agreement. The degree of fit is at least as good as, if not better than, that achieved by Tavare et al. using the model of Liao and Hulburt. As a further check of the model used here, the experimental and calculated magma densities may be compared. The third moment of the population density function, calculated from the numerical solution, is computed to be $m_3 = 86.5 \times 10^{12}$ μm$^3/L$ which implies a magma density of $M_T = 87.1$ kg/m^3. This calculated value compares very well with the experimental value of $M_T = 91.0$ kg/m^3, exhibiting an error of 4.3%. The equivalent density calculated by the model-fit of Tavare et al. is $M_T = 100.1$ kg/m^3, which is in error by 10.0%.

The nucleation and growth rates calculated from the DPB are some three times greater than those calculated by Tavare et al., $B_0 = 0.654 \times 10^9$ 1/h · L, and $G = 130.6$ μm/h. Some insight into why this might be so may be afforded by examination of an index of aggregation.

$$I_{Agg} = 1 - \frac{\text{No. of crystals leaving the vessel}}{\text{No. of crystals nucleated}}$$

$$= 1 - \frac{m_0}{\tau B_0} \tag{37}$$

Using this index, systems in which little aggregation occurs have values of $I_{Agg} = 0$. Conversely, systems in which much aggregation occurs have values of I_{Agg} near 1.

It may be shown that the zeroth moment calculated from the model of Liao and Hulburt is given by

$$m_0 = \sqrt{\frac{2B_0}{A}}\left(\frac{\sqrt{P+1} - \sqrt{P-1}}{\sqrt{P+1} + \sqrt{P-1}}\right)$$

where

$$P = \sqrt{1 + \frac{1}{2AB_0\tau^2}}$$

Using this last result it is possible to calculate the aggregation index implied by the estimated parameters of Tavare et al. as $I_{Agg} = 0.487$. Using the DPB and the appropriate moment generating function, Eq. 14, the value of the aggregation index is 0.857. It seems, then, that analysis based on the full population

balance, rather than the approximate, length-conserving model, indicates a substantially greater loss of crystal numbers by aggregation. It thus follows that the nucleation rate calculated by Tavare et al. must be lower than that calculated here, if the calculated total number of crystals leaving the reactor is to be correct. It now only remains to explain why the growth rate calculated in the present work is greater than that calculated by Tavare et al.

In fitting a three-parameter model, such as either of the population balances under discussion here, to cumulative over-size data, one may interpret the process as being a matter of matching predicted and experimental values for the axis intercept, COS(0), the slope at the intercept, $d/dL\text{COS}\ (L)|_{L\sim 0}$ and the curvature or shape of the plot. The axis intercept, COS (0), is equal to m_0, which in both cases is determined by the aggregation parameter, β_0 or A, and the nucleation rate B_0. The slope at $L = 0$ is $d/dL\ \text{COS}\ (L)|_{L\sim 0} = -n(0)$, which for Liao and Hulburt's problem is B_0/G. It is well understood that the shape of the plot depends on the aggregation parameter. One obvious demonstration of this point is that the plot is a straight line when no aggregation occurs.

We have seen already that in order to predict correctly the axis intercept, the nucleation rate calculated from the DPB must be greater than that calculated from Liao and Hulburt's model. The same approach applied to the slope at the intercept explains the difference in growth rates. As a first approximation it may be assumed that this slope is given by B_0/G for all cases. Thus, if the values of B_0 differ, then so must the values for G. Tavare et al. find that $B_0/G = 5.00 \times 10^6$, while for the current study, $B_0/G = 4.29 \times 10^6$. These values are probably within the tolerance expected from parameter estimation and the accuracy of the foregoing assumption concerning the constancy of the ratio.

If the discrete approach is accepted as providing the correct solution to the appropriately formulated problem, that is, one in which aggregation conserves volume, not length, one may conclude that the approximations inherent in the analysis of Liao and Hulburt lead, in this case at least, to a substantial underestimation of the growth and nucleation rates.

Conclusions

- The discretized population balance developed by Hounslow et al. (1988a) for batch systems has been employed in the analysis of continuous systems at steady state.
- The discretized population balance has been compared with the analogous continuous equation and has been shown to be equivalent for nucleation, growth, and aggregation. Both size-dependent and size-independent kinetics have been studied; in every case the two forms of the population balance were found to be equivalent.
- A criterion for selecting the extent of the discrete size domain has been developed.
- The equation-oriented flowsheeting package, SpeedUp, has been used to model a continuous mixed-suspension mixed-product-removal crystallizer. The parameter estimation facilities of SpeedUp have been used to determine the kinetic rate parameters for a system undergoing simultaneous nucleation, growth, and aggregation.
- It has been shown that the approach of Liao and Hulburt (1976) to the analysis of a crystal-size distribution from a CMSMPRC in which nucleation, growth, and aggregation are active, leads to the underestimation of the nucleation and growth rates.

Acknowledgment

This work was supported by a project grant from the National Health and Medical Research Council of Australia and a grant-in-aid from the University of Adelaide.

Notation

A = Aggregation parameter in the model of Liao and Hulburt (1976)
a, b, c = constants in Eq. 17
b = parameter in the model of Abegg et al. (1968)
B = birth rate, $1/\mu\text{m} \cdot L \cdot \text{h}$
B_0 = nucleation rate, $1/L \cdot \text{h}$
COS = cumulative oversize
f = normalized population density function
FDE = finite domain error
g = a function
D = death rate, $1/\mu\text{m} \cdot L \cdot \text{h}$
G = linear rate of growth, $\mu\text{m/h}$
h = a function
I_{Agg} = index of aggregation
L = particle size
L_i = lower bound of the ith size interval
m_j = jth moment, $\mu\text{m}^j/L$
n = population density function, $1/\mu\text{m} \cdot L$
n_{eq} = number of discrete size intervals
n_t = number of terms in series solution
N = cumulative number undersize, $1/L$
N_0, v_0 = parameters in Eq. 30
N_i = number of particles in the ith interval, 1/L
N_T = total crystal number per volume of suspension, 1/L
$\bar{N}$ = dimensionless number of particles in the range L to rL
p_i = polynomial coefficient
P = parameter in the model of Liao and Hulburt (1976)
Q = volumetric flow rate, L/h
r = ratio, L_{i+1}/L_i
SSE_5 = sum of square error, as defined in Eq. 20
t = time, h
T = dimensionless time
v = crystal volume, μm^3
V = volume, L
$\underset{\sim}{x}$ = coordinate vector
x = dimensionless size

Greek letters

α = constant in the Euler transformation, Eq. 2.4
β = aggregation kernel, L/h
β_0 = size-independent portion of the aggregation kernel, L/h
δ = dirac delta function
ϵ = variable of integration, volume
λ = variable of integration, length
τ = draw-down time
ζ = conserved property

Literature Cited

Abegg, C. F., J. D. Stevens, and M. A. Larson, "Crystallization Size Distributions in Continuous Crystallizers When Growth Rate is Size Dependent," *AIChE J.*, **14**(1), 118, (1968).

Abramowitz, M., and I. E. Stegun, *Handbook of Mathematical Functions*, 9th printing, p. 1024, Dover Publications Inc., New York (1960).

Batterham, R. J., J. S. Hall, and G. Barton, "Pelletizing Kinetics and Simulation of Full Scale Balling Circuits," *Proc. 3rd Int. Symp. on Agglomeration*, Nürnberg, W. Germany, A136 (1981).

Domb, C. and M. F. Sykes, "Susceptibility of a Feromagnetic Above the Curie Point," *Proc. Roy. Soc. Ser. A*, **240**, 214 (1957).

Gelbard, F., and J. H. Seinfeld, "Numerical Solution of the Dynamic Equation for Particulate Systems," *J. Comp. Phys.* **28**, 357 (1978).

———, "Simulation of Multicomponent Aerosol Dynamics," *J. Colloid and Interf. Sci.*, **78** (2), 485 (1980).

Gelbard, F., Y. Tambour, and J. H. Seinfeld, "Sectional Representations for Simulating Aerosol Dynamics," *J. Colloid and Interf. Sci.*, **76** (2), 541 (1980).
Hearn, A. C., *Reduce User's Manual*, The Rand Corporation, Santa Monica (1984).
Hounslow, M. J., R. L. Ryall, and V. R. Marshall, "A Discretized Population Balance for Nucleation, Growth, and Aggregation," *AIChE J.*, **34** (11), 1821 (1988a).
———, "Modelling the Formation of Urinary Stones," *CHEMECA 88*, 1097, Sydney, Australia (1988b).
Hounslow, M. J., "Solving the Population Balance," *Int. Symp. on Agglomeration*, Brighton, England, 585 (1989).
Hulburt, H. M., and S. Katz, "Some Problems in Particle Technology: A Statistical Mechanical Formulation," *Chem. Eng. Sci.*, **19**, 555 (1964).
Liao, P. F., and H. M. Hulburt, "Agglomeration Processes in Suspension Crystallization," *Annual Meeting of AIChE*, Chicago (Dec., 1976).
Marchal, P., R. David, J. P. Klein, and J. Villermaux, "Crystallization and Precipitation Engineering—I. An Efficient Method for Solving Population Balance in Crystallization with Agglomeration," *Chem. Eng. Sci.*, **43** (1), 59 (1988).
Ramkrishna, D., "The Status of Population Balances," *Rev. in Chem. Eng.*, **3** (1), 49 (1985).
Randolph, A. D., and M. A. Larson, *Theory of Particulate Processes*, 2nd ed., Academic Press (1988).
Prosys Technology Ltd., *The SpeedUp User Manual*, Prosys Technology Ltd., Cambridge (1988).
Sargent, R. W. H., J. D. Perkins, and S. Thomas, "SPEEDUP: Simulation Program for the Economic Evaluation and Design of Unified Processes," *Computer-Aided Proc. Plant Des.*, M. E. Lesley, ed., Gulf Publishing, Houston (1982).
Tavare, N. S., M. B. Shah, and J. Garside, "Crystallization and Agglomeration Kinetics of Nickel Ammonium Sulphate in an MSMPR Crystallizer," *Powder Technol.*, **44**, 13 (1985).
Van Dyke, M., *Perturbation Methods in Fluid Mechanics*, The Parabolic Press, Stanford (1975).

Appendix 1: Solution for size-independent aggregation

Equation 31 may be rearranged to give

$$f(x) = \frac{T}{2\sqrt{1+2T}}\int_0^x f(x-\epsilon)f(\epsilon)\,d\epsilon + \frac{e^{-x}}{\sqrt{1+2T}}$$

Taking the Laplace transform with respect to x, yields

$$\bar{f}(s) = \frac{T}{2\sqrt{1+2T}}\bar{f}(s)^2 + \frac{1}{(s+1)\sqrt{1+2T}}$$

solving for $\bar{f}(s)$, and keeping the appropriate root,

$$\bar{f}(s) = \frac{1}{T}\left(\sqrt{1+2T} - \sqrt{\frac{(1+2T)s+1}{s+1}}\right) \qquad (1.1)$$

Consider the related function, $g(x)$, which has a Laplace transform

$$\bar{g}(s) = \sqrt{\frac{As+1}{s+1}} \quad A \in R$$

$$= \sqrt{A}\,\frac{s+1/A}{\sqrt{s+1}\,\sqrt{s+1/A}}$$

Designating part of this expression as $\bar{h}(s)$, where

$$\bar{h}(s) = \frac{1}{\sqrt{s+1}\,\sqrt{s+1/A}}$$

then, from Abramowitz and Stegun (1965)

$$h(x) = \exp\left(-(1+1/A)\frac{x}{2}\right) I_0\left((1-1/A)\frac{x}{2}\right)$$

now, $s\bar{h}(s) = \mathcal{L}(h') + h(0)$, and $h(0) = 1$, so the inverse of this relationship is

$$\mathcal{L}^{-1}(s\bar{h}) = h' + \delta(x) \qquad (1.2)$$

Comparing g and h,

$$\bar{g}(s) = \sqrt{A}\,s\bar{h} + \frac{\bar{h}}{\sqrt{A}}$$

By 1.1

$$g(x) = \sqrt{A}\left(\frac{dh}{dx} + \frac{h}{A} + \delta(x)\right)$$

$$= \delta(x)\sqrt{A} - \frac{A-1}{\sqrt{A}}\exp\left[-(1+1/A)\frac{x}{2}\right]$$

$$\left(I_0\left[(1-1/A)\frac{x}{2}\right] + I_1\left[(1-1/A)\frac{x}{2}\right]\right) \qquad (1.3)$$

Now, 1.1 may be rewritten as

$$\bar{f}(s) = \frac{1}{T}\left(\sqrt{1+2T} - \bar{g}|_{A=1+2T}\right) \qquad (1.4)$$

Which, by use of 1.3, may be inverted, yielding

$$f(x) = \frac{1}{T}\left(\delta(x)\sqrt{1+2T} - g|_{A=1+2T}\right)$$

$$= \frac{I_0\left[\frac{-Tx}{1+2T}\right] + I_1\left[\frac{-Tx}{1+2T}\right]}{\exp\left[\frac{-(1+T)x}{1+2T}\right]\sqrt{1+2T}}$$

Appendix 2: Solution for size-dependent aggregation

If a new function, $g(x)$, is defined by $f = e^{-x}g$, then after dividing through by e^{-x}, Eq. 36 becomes

$$0 = \frac{1}{2}\int_0^x xg(x-\epsilon)g(\epsilon)\,d\epsilon$$

$$- g(x)\left(\frac{x}{1+T} + 1\right) + \frac{1-g}{T} \qquad (2.1)$$

Equation 2.1 cannot be solved by the method of Laplace transforms; an attempt to do so results in a first-order nonlinear ordinary differential equation in the s domain.

Picard's method was used to develop a series form of $g(x)$, given by

$$g(x) = \sum_{i=0}^{n_t} p_i x^i \tag{2.2}$$

Equation 2.1 was first rearranged to give

$$g(x) = \frac{T}{T+1}\frac{x}{2}\int_0^x xg(x-\epsilon)g(\epsilon)\,d\epsilon - g(x)\frac{xT}{(1+T)^2} + \frac{1}{T+1} \tag{2.3}$$

Then, using $p_0 = 1/T + 1$ as a starting estimate, additional terms in 2.2 were determined by direct substitution in 2.3. The integration and algebraic manipulation required to evaluate 2.3, were carried out using the computer package REDUCE (Hearn, 1984). It should be noted that the values of the coefficients, p_i, were maintained in a numeric form, not an algebraic one. Consequently, the coefficients were determined separately for each value of T of interest.

The solutions generated by Picard's method for this problem cannot be used directly—the series are not convergent for large values of x. The coefficients, p_i, are of alternating sign which is indicative of a singularity on the negative real axis with a consequent finite radius of convergence along the positive real axis. Van Dyke (1975) describes the use of the Euler transformation to overcome this problem. The variable x is replaced by u, defined as

$$x = \alpha\left(\frac{u}{1-u}\right) = \alpha\sum_{i=1}^{n_t} x^i \tag{2.4}$$

Substituting 2.4 into 2.2 yields another series solution for g, which by careful selection of α, might be convergent. The effect of the Euler transformation is to map $(-\alpha, +\infty)$ onto $(-\infty, +1)$, so that a singularity at $-\alpha$ on the real axis is now located at $-\infty$ and the radius of convergence about 0 is increased to $u = 1$, that is, $x = \infty$.

For $T = 1$, an apparently convergent solution may be deduced with $\alpha = 10$ and the number of terms, n_t, equal to 25. For $T = 0.25$, $\alpha = 0.02$ and $n_t = 25$ gave apparently good results. A series was accepted as giving a useful solution when the calculated size-distribution possessed a single mode and the associated zeroth moment stabilized to a value near $1/T + 1$.

While the values for α were chosen on a trial and error basis, some rationalization of their magnitude is possible. If the dominant singularity on the negative real axis is at ϵ, an appropriate value for α is $\alpha = -\epsilon$. Using the method of Domb and Sykes, the nearest singularities were determined as $\epsilon = -63$ and -4.0 for $T = 0.25$ and 1.0, respectively. Why, for $T = 1$, $\alpha = 10$ gives a better value than $\alpha = 4$, is not clear. It is even less clear why a small value of α should give better results than the expected large value for $T = 0.25$.

Manuscript received Mar. 20, 1989, and revision received Oct. 20, 1989.